Wetting Transition on Hydrophobic Surfaces Covered by Polyelectrolyte Brushes

Pierre Muller, Guillaume Sudre, Olivier Theodoly

Wetting transition on hydrophobic surfaces covered by polyelectrolyte brushes.

P. Muller[a, b] , G. Sudre[a], O. Théodoly[a, c *]

[a] *Complex Fluids Laboratory, CNRS UMR 166, 350 George Patterson Blvd, Bristol PA 19007, USA.*
[b] *Université Strasbourg 1, Institut Charles Sadron, CNRS UPR 22, 23 rue du Loess, BP84047, F-67034 Strasbourg Cedex 2*
[c] *Laboratoire Adhésion et Inflammation, INSERM U600, CNRS UMR 6212, Case 937, 163 Avenue de Luminy, Marseille F -13009, France ; Aix-Marseille Université, Faculté des Sciences/de Médecine ou de Pharmacie, Marseille, F -13000, France.*

*corresponding author. Tel.: +33 (0)4 91 82 88 69; Fax: Tel.: +33 (0)4 91 82 88 50.
email: Olivier.theodoly@inserm.fr

Keywords: polyelectrolyte, wetting, Young-Dupré equation, polymer brush, interfacial tension.

ABSTRACT: We study the wetting by water of complex "hydrophobic-hydrophilic" surfaces made of a hydrophobic substrate covered by a hydrophilic polymer brush. Polystyrene PS substrates covered with polystyrene-block-poly(acrylic acid) PS-b-PAA diblock copolymer layers were fabricated by Langmuir-Schaefer depositions and analyzed by AFM and ellipsometry. On bare PS substrate, we measured advancing angles $\theta_A = 93 \pm 1°$ and receding angles $\theta_R = 81 \pm 1°$. On PS covered with poorly anchored PS-b-PAA layers, we observed large contact angle hysteresis, $\theta_A \approx 90°$ and $\theta_R \approx 0°$ that we attributed to nanometric scale dewetting of the PS-b-PAA layers. On well-anchored PS-b-PAA layers that form homogeneous PAA brushes, a wetting transition from partial to total wetting occurs versus the amount deposited: both θ_A and θ_R decrease close to zero. A model is proposed, based on the Young-Dupré equation, that takes into account the interfacial pressure of the brush Π, which was determined experimentally, and the free enthalpy of hydration of the polyelectrolyte monomers ΔG_{PAA}^{hyd}, which is the only fitting parameter. With $\Delta G_{PAA}^{hyd} \approx -1300$ J/mol, the model renders the wetting transition for all samples and explains why the wetting transition depends mainly on the average thickness of the brush and weakly on the length of PAA chains.

1. Introduction

Practical and durable hydrophilization of hydrophobic substrates is a on-going field of research motivated by academic and industrial interests. Non-woven polypropylene tissues are naturally hydrophobic and have to be hydrophilized to absorb water (wipes), or let water go through (diapers). For surface cleaning (windshield, glasses, windows, cars), hydrophilizing the surface permits to avoid, upon drying, the formation of drops that let unaesthetic stains. A simple solution to hydrophilize a surface consists in depositing amphiphilic molecules. However, small-molecule surfactants have the disadvantage of being easily washed-out upon first contact with water. Polymeric amphiphilic molecules are therefore an interesting alternative to achieve more durable hydrophilizing treatments at low cost. The quality of such treatments will depend on the stability of the polymer layer at the surface (*against* washing, drying, rubbing, aging, etc…), and of the efficiency of the hydrophilization, *i.e.* the increase of the surface energy. Several routes permit to improve the stability of the polymer layer. One route relies on adhesion, which is maximized with a higher affinity between the surface and the hydrophobic polymer moieties and also with polymers of larger molar mass. Another route consists in anchoring the polymeric layer to the surface, either physically or chemically. For the hydrophilization efficiency, one may expect that covering a hydrophobic substrate with a highly hydrophilic layer is enough to make the surface totally wetting. However, a hydrophilic layer is by essence not waterproof, and does not hamper the contact between the hydrophobic substrate and water. It is not obvious to infer what shall be the thickness and/or density of the hydrophilic layer necessary to overcompensate the presence of the underlying hydrophobic layer. The question tackled in this paper can be stated as: what governs the wetting by water of a complex surface made of a hydrophobic substrate covered by a hydrophilic polymer? A pioneer theoretical work was published in 1984[1], and later improved[2], on the wetting of a pure non volatile solvent on a solid coated by an uncharged polymer. In good solvent conditions, it

is predicted that the entropy of dissolution of the polymer for usual brushes (polymerization length 100, grafting density 0.01 chain.Å^{-2}) drives the spreading parameter, leading to conditions of total wetting. Later, experimental and theoretical works have treated the case of a polymer brush in contact with a liquid polymer made up of the same monomers as the brush[3,4,5,6,7], with a mixture of solvents[8] , and with a nematic fluid[9]. The wetting by a simple fluid (water) of a hydrophilic uncharged brush grafted on a hydrophobic substrate was only considered recently[10]. It was demonstrated that a transition to complete wetting could not be obtained with poly(ethylene oxide) PEO brushes. This result was attributed to a bridging of the solvent-vapor interface by the grafted layer. In the present study, we consider the wetting by a simple volatile fluid (water) of a polyelectrolyte brush. We use model hydrophobic substrates made of polystyrene spin-coated on atomically flat silicon wafers. The grafted hydrophilic polymer brushes are made with diblock copolymers of polystyrene PS and poly(acrylic acid) PAA. PS permits a physical anchoring of the chains to the substrate, whereas PAA is a strongly hygroscopic polyelectrolyte, which is routinely used for super-absorbent properties. The surface treatments are performed by the Langmuir-Schaefer technique (transfer from air/water to PS-water interface) followed by an annealing procedure to anchor the brush. The state of the brushes is characterized by ellipsometry and AFM. The contact angles with water are finally measured *versus* the amount of PAA deposited and the length of the PAA chains. A thermodynamic model is then proposed to interpret the wetting properties of complex surfaces made of a hydrophobic substrates covered by a hydrophilic polymer brush.

2. Experimental Section

Materials. Silicon wafers (thickness 281µm +/- 25µm, orientation (100), no dopant, RMS roughness measured by AFM at 5 Å on 1x1 mm images) were purchased from Silicon Inc., Hexamethyldisilasane (HMDS) from Gelest, Inc., polystyrene (Primary Standard polystyrene M_w=350,000g/mol) from TSK, and polystyrene-block-poly(acrylic acid) PS-b-PAA samples from Polymer Source Inc. The PS-b-PAA samples used in this study have molar masses of 1.8K-6K, 1.5K-44K, 4.5K-19.3K and polydispersity indexes lower than 1.1.

Preparation of PS substrates. Silicon wafers are first cleaned in a UV/O_3 chamber for 15 min and immediately silanized with HMDS in vapor phase for 2 hours at ambient pressure and temperature. This pre-treatment is required to avoid problems when the PS layer is put in water solutions. Without this pre-treatment, small pockets of water appear between the PS layer and the hydrophilic wafer surface. PS layers are then spin-coated at 5,000 RPM for 1 min from a PS solution in toluene filtered at 0.2 µm and at concentration 2.5 wt%. The layers are finally annealed overnight at 80 ºC. The average thickness of the PS layer is measured by ellipsometry around 120 nm. The average RMS roughness measured by AFM is around 0.6 nm for 1 micron square.

Langmuir trough isotherms. Compression isotherms of PS-b-PAA copolymers at the air/water interface have been measured on a commercial Langmuir trough (model NIMA 611). A known amount of PS-b-PAA samples is dissolved at a concentration of 1 mg/g in a solvent made of 1,4-dioxane with HCl at 2 wt%. This solvent is a good compromise between good spreading properties at the air/water interface, which is easily achieved with apolar solvents, and good solvency properties for PAA-rich diblock samples, which can be achieved with polar solvents. A few microliters of diblock solutions are spread drop by drop onto the water surface with a micro syringe (Hamilton). Since dioxane is miscible with water, part of the material may sink in the water subphase. The absolute amount deposited has to be measured *a posteriori* by ellipsometry.

Langmuir-Schaefer depositions. The monolayers are transferred from the air/water interface to the PS substrate by the Langmuir-Schaefer technique[11], which consists in stamping the PS substrate face-down across the air/water interface. The monolayer at the air/water interface is removed by aspiration in order to avoid the deposition of a second layer on the substrate during its removal from the trough. The samples with the depositions are stored in water. Caution was taken to maintain the sample wet and avoid strong shear flows during all manipulations to avoid damaging the deposited monolayers. Each transferred layer is identified by the surface pressure at which the transfer is performed. As explained above, the area per molecule calculated based on the amount of material dissolved in the spreading solution is subject to uncertainty, whereas a given surface pressure Π characterizes a unique surface layer concentration. For very dilute layers, when the slope of the surface pressure *versus* the surface concentration is small, the control of the amount of transferred copolymer per unit area at a given surface pressure Π is less precise. For this reason, we decided to proceed differently for depositions at surface pressures Π lower than 2.5 mN/m. A layer was first compressed to a surface pressure of 2.5 mN/m, then the area was increased by a factor Y. Deposition prepared by this method are labeled 2.5mN/m:Y. Three dilute layers have been prepared, 2.5mN/m:3, 2.5mN/m:5, and 2.5mN/m:8.

Anchoring of deposited layers. Two methods have been used to anchor the deposited PS-b-PAA monolayers on the PS substrates. The toluene swelling method consists in adding toluene to the water in which the samples are stored. In order to control the amount of toluene in water, we prepared mixtures of pure water and water saturated with toluene. We call X the mass percent of toluene-saturated water in a mixture. The samples with a deposited diblock monolayer were let for 1 min in a water-toluene solution with X = 40%. The water-toluene solution was then exchanged by pure water and the samples were finally dried with a gentle flow of pure nitrogen. Alternatively, the temperature annealing method consisted in increasing the water temperature in which the samples are stored. The samples were left in water at 60 ºC for 19 hours, then cooled down and dried with nitrogen.

Contact angle measurement. Side pictures of drops on the substrates were taken on a home-made goniometer and contact angles were measured by fitting the edges of drops with the DropImage software (Rame Hart, Mountain Lake, NJ). The precision is of ±1° and the lowest measurable angle is around 10°. The volume of the drop was manually tuned with a precision syringe in order to measure the advancing contact angle θ_A (highest stable angle observed when the drop volume is increased) and the receding contact angle θ_R (lowest stable angle observed when the drop volume is decreased).

Ellipsometry. We used a multi-wavelength ellipsometer MOSS model ESVG (SOPRA, France). Measurements were taken at wavelengths between 250 nm and 600 nm, and at an incidence angle of 70°. For analysis, we used the WinElli software (SOPRA, France), that considers flat and homogeneous multilayers. The refractive index and thickness of the native silica layer on the silicon wafers is measured on a bare substrates. The refractive index as function of the wavelength for PAA and PS materials were determined experimentally on thin layers of homopolymers PAA and PS spin coated on a silicon wafer. The initial thickness of the substrates of PS is measured for each sample, prior to the Langmuir-Schaefer deposition. These data are introduced as fixed parameters in the subsequent multilayer models used to determine the thickness of deposited PS-b-PAA monolayers. All ellipsometric measurements are performed in the dry state.

AFM. A Nanoscope III AFM (from Digital Instrument, now Veeco) in the tapping mode was used to investigate the structure of the deposition in air. We used Silicon cantilevers NSC35/AIBS/50 from Micro Mash.

3. Results and Discussion

Isotherms. The isotherms for all the diblock copolymers on pure water are reported on Figure 1. The increase of pressure with surface density is smooth, which is an indication that the hydrophobic PS block does not participate to the surface pressure. Homopolymer of PS isotherms are typically flat up to a limiting area, with a sudden pressure rise from that point. They are also characterized by irreversible collapse. The small mass fraction of PS in the copolymer studied insure that the hydrophobic block never completely cover the air/water interface. It is thus natural to assume that the surface pressure is only due to the hydrophilic part of the diblock. The area per molecule is calculated from the concentration of the solution deposited, the volume of solution deposited, and the surface of the air/water interface. Several consecutive compressions and expansions for a given deposition superpose on a single curve, which means that diblock copolymers are well anchored at the air/water interface. Figure 1 reports isotherms for different deposited amounts. Between measurements taken with different deposited amounts, a multiplicative factor is applied to the abscises in order to merge all data corresponding to a same copolymer on a single curve. The need of a multiplicative factor shows that the deposition of material at the air/water interface is not exactly reproducible. The reason comes from the use of dioxane as spreading solvent. Dioxane is miscible with water at all concentration so that some material is lost in the subphase upon deposition. The calculated area per molecule on Figure 1 is only defined within a multiplicative constant. The absolute area per molecule has to be determined by ellipsometry measurement done after transfer onto solid substrate. These absolute values are also needed for a precise physical understanding of the isotherms characteristics, which is out of the scope of the present work and is presented elsewhere[12]. Isotherms are used here as a mean to prepare polymer monolayer on solid substrates in a controlled manner.

Anchoring. A gentle flow of water is sufficient to desorb the monolayer transferred on PS substrates. This is detected by contact angle measurements (contact angles with water increase with the number of rinsings) and ellipsometric measurements (the deposited layer thickness falls down to zero after rinsing). We also remarked that drying the samples without any anchoring procedure was damaging for the copolymer monolayers and changed the wetting properties. This has two implications. First, anchoring the brush to the PS substrates is a prerequisite to wetting measurement with water. And second, since samples after Langmuir-Schaefer deposition are wet and drying damages the samples, the anchoring method must be performed in the wet state. The idea of the toluene method is to swell the PS sublayer and allow the PS block of copolymers to penetrate the PS sublayer[13], as cartooned on Figure 2-a-

b. When toluene is removed, the PS sublayer contracts back and traps the diblock chains. Note that cartoons of Figure 2-a-b illustrate the interpenetration of PS chains and does not pretend to represent the organization of the PAA chains[14]. In order to optimize the toluene method, the PS layer thickness *versus* the content of toluene was measured by ellipsometry in immersed conditions (Figure 2-b). The thickness increases by less than 5% for toluene-water solutions with X lower than 50%, and diverges for X above 60% (the PS layer is dissolved). In this work, mixtures at X = 40% were used for anchoring the diblock copolymers. The PS layers swell by 3.5% without damage for the PS layer, as checked by AFM imaging before and after treatment (average RMS roughness is 0.6 nm in both cases). With the diblock monolayer, we found great improvement of the anchoring against drying. Figure 3 compares AFM images of dry PS-b-PAA 4.3k-19.5k layers deposited at Π = 4.5mN/m., for different anchoring conditions. The average thickness of the layers measured by ellipsometry are comparable for the three samples. The anchored layers (Figure 3-b and c) appear featureless and have an average RMS roughness of 0.85 nm. On the contrary (Figure 3-a), the non-anchored layer shows heterogeneities and has an average roughness of 1.5 nm. Differences are also detected by contact angle measurements that lead to lower angles and smaller hysteresis for the anchored samples. Anchoring strength is also improved against rinsing. Repetitive contact angles give higher and higher values on non treated samples, indicating a washing of the deposited diblock layer, whereas constant values are found on treated samples for at least 5 consecutive measurements. Note that the toluene anchoring method works only for a narrow window of toluene concentration (around X = 40%) and treatment time (around 60 s). For lower X values or shorter treatment time, anchoring is too weak, whereas for higher X values or longer treatment time, the depositions layers were damaged. Although the toluene swelling method was found efficient for most deposition conditions, we found that they induce instabilities of deposited layers at low surface concentration. Figure 4 shows AFM pictures of deposited layers that have been treated by the toluene method and that present typical patterns of a monolayer dewetting. This interpretation is confirmed by the thickness difference between the dark and bright zones on the picture (4-5 nm) that correspond to the average layer thickness measured by ellipsometry (3.5-4.7 nm). For low concentration depositions, we therefore preferred the temperature annealing method, at 60 ºC for 19 hours. With this method, all deposited layers at 4.5 mN/m are featureless and have an average RMS roughness of 0.7 nm.

Ellipsometric calibration of deposited monolayers. The actual amount deposited on the wafer was systematically determined by ellipsometry. Two fitting models have been tried. Model 1 considers the diblock layer as a homogeneous PAA layer, whose thickness h_1 is the only fitting parameter. Model 2 considers the PS subphase and the deposited diblock layer as two superposed layers of PS and PAA of thicknesses h_2^{PS} and h_2^{PAA}. An example of ellipsometric measurement before and after deposition of a layer of PS-b-PAA 1.8k-6k deposited at 21 mN/m is presented on Figure 5. The one parameter fit for the thickness of the PS substrate gives 118.7 nm. Models 1 and 2 lead to fittings of equivalent quality and yield consistent results in terms of total thickness. Table 1. Model 1 is reported on Figure 5 and used for all results presented in the following.
Ellipsometry thickness $e_{ellipso}$ of deposited layers for the three diblock samples deposited at different surface pressures are reported on Figure 6 *versus* the langmuir thickness $e_{Langmuir}$ calculated based on the number of molecule per angstrom square used to plot the isotherms of Figure 1. The dependence is remarkably linear for the three samples. This proves that the effective transfer rate upon the Langmuir-Schaefer transfer and the anchoring process is constant, otherwise, the data of Figure 6 would be random. On the other hand, the ellipsometric amounts are 2.59, 2.86 and 3.40 times smaller for respectively PS-b-PAA 1.8k-6k, 4.3k-19.5k, and 1.5k-44k, as compared to the amounts deposited on the Langmuir trough. This is explained by a loss of material upon deposition of copolymer with dioxane solutions. In any case, ellipsometry permits to access the exact amount of diblock present on the solid substrates and to recalibrate the areas of the isotherm data. We have checked that the correction does not change the relative position of the isotherms for the three diblocks on Figure 1. One can conclude that the pressure increases expectedly with the molar mass of the PAA block at a given area per molecule[12].

AFM imaging of deposited monolayers. The topography of deposited and anchored monolayers was systematically checked by AFM. For depositions made at surface pressures above 4.5 mN/m, the samples are generally flat and featureless with RMS values around 0.5-0.7 nm, as shown on Figure 7. Macroscopic cracks are occasionally observed in deposition made at the pressures larger than 20 mN/m. These defects, visible with the naked eye, are an opportunity to get more insight into the structure of the layers via AFM imaging. Figure 8-a presents the image of a crack in a PS-b-PAA 4.3k-19.5k deposited at 25 mN/m and Figure 8-b presents a height profile taken on the same image. One can clearly identify three different levels. As cartooned on the profile, these levels correspond to the bare PS substrate, the diblock monolayer, and a diblock trilayer formed by local collapse of the monolayer. The cracks

and collapses probably form during the Langmuir-Schaefer transfer. The monolayer zone is very flat (RMS = 0.27 nm), which shows that the carpet of PAA chains is dense and homogeneous. We note also that the thickness of the monolayer measured by AFM (10.5 nm) is remarkably consistent with the ellipsometric measurement (10.3 nm). The case of depositions made at pressures lower than 4.5 mN/m is different. Figure 4 shows that layers deposited at 4.5 mN/m and anchored by the toluene method present topographic heterogeneities that result from a dewetting of copolymer monolayer. At the opposite, Figure 9-a shows that the same deposition at 4.5 mN/m anchored by the temperature method are flat and homogeneous. The temperature method is clearly more appropriate to anchor the low density layers. Nevertheless, at 2.5mN/m (Figure 9-b), heterogeneities appear at the surface even with the temperature annealing method. On samples 2.5mN/m:3 (Figure 9-c) and 2.5mN/m:5 (Figure 9-d), we observe circular objects of diameter around 50 nm, which are attributed to surface micelles. At 2.5mN/m:8 (not shown) there are no features anymore. It is out of the scope of this paper to find out if the micelles observed on the transferred layers are due to the transfer/anchoring process or to organizations already present at the air/water interface. This study of the spontaneous formation of micelles at the air/water interface is presented elsewhere[14].

Wetting data. The measured contact angles on the bare PS substrates are $\theta_a = 93° \pm 1$ and $\theta_r = 81° \pm 1$. Figure 10 presents the contact angle *versus* the thickness of acrylic acid anchored e_{AA} for all samples with homogeneous PS-b-PAA layers, *i.e.* for depositions made at pressures above 4.5 mN/m and annealed by the "toluene route". The thickness e_{AA} of dry acrylic acid layer for a PS-b-PAA λk-μk layer of ellipsometric thickness $e_{ellipso}$ is calculated as $e_{AA} = e_{ellipso} \cdot \frac{\mu}{\lambda+\mu}$ (where λ and μ are the molar masses in kg/mole of the PS and PAA block respectively), which assumes comparable densities for the two polymers. All receding angles are smaller than the experimental limit of 10° and all the samples remain wet after complete aspiration of a drop. For the advancing angles, there is a transition from very low advancing angles (15-25°), that form a plateau at high PAA thickness, to high advancing angles (50-60°) at low PAA thickness. The hysteresis between the advancing and receding contact angles is important. It is interesting to remark that hysteresis of contact angles have also been measured with PS-b-PAA layers that are not properly anchored. However, wetting behavior on such substrates is quite different. The receding contact angles can be close to zero for high PAA thickness, whereas the advancing contact angles are always close to 90°. Dewetting of the PS-b-PAA layer into small caps of 20-50 nm distant by 50-100 nm have been clearly identified by AFM imaging of dry samples. The hysteresis in this case is due to the chemical heterogeneity of the surface, the areas of bare PS explaining the high advancing contact angles. In the case of Figure 10, the contact angle hysteresis can not be attributed to chemical heterogeneities because AFM characterizations have shown that the surface of dry samples consist of dense and homogeneous carpet of PAA. On Figure 10, the PAA thickness at which the transition of advancing angles occurs is indicated by horizontal bars a, b, and c for respectively PS-b-PAA 1.8k-6k, 4.3k-19.5k, and 1.5k-44k. The edges of bars a, b and c correspond to the highest e_{AA} with θ_A above the plateau of small angles, and the lowest e_{AA} with θ_A at the plateau of small angles. Despite the scarcity of data point and the width of the bars, it appears that the transition of advancing angles occurs at higher PAA thickness for copolymers of longer PAA blocks. This suggests that for a given amount of PAA, PAA carpets with dense and short hair induce less hysteresis than carpets with scarce and long hair. It is then tempting to attribute this hysteresis to surface heterogeneities at the molecular level. Let us now present the contact angle measurements for PS-b-PAA 4.3k-19.5k for all depositions, either annealed by the temperature or the toluene route (Figure 11). We decided to present these data on a separate plot because they correspond to some layers that are homogeneous and others that are heterogeneous. Still, it appears that there is a good continuity between results for all layers. A clear wetting transition from partial wetting to total wetting is visible on both advancing and receding angles around 3.5 to 4.5 nm of PAA thickness.

Model. Figure 12 presents a cartoon of a water drop on a hydrophobic substrate covered with a polyelectrolyte brush. The brush is collapsed and dry when exposed to air and hydrated and swollen underneath the drop. Following the reasoning of the Young-Dupré equation[15],[16],[17], we evaluate the infinitesimal work dW involved in the displacement of the triple contact line on such a complex surface. One can express dW as:

Eq. 1

$$dW = ((\gamma_{PS-H_2O} - \gamma_{PS-PAA})(1-\sigma) + \gamma_{H_2O-air} \cdot \cos\theta + W_{PAA}^{hyd} - \gamma_{PAA-air}) \cdot dA$$

where $\gamma_{PS\text{-}H2O}$ is the interfacial energy between PS and water, $\gamma_{H2O\text{-}air}$ between water and air, $\gamma_{PAA\text{-}PS}$ between PS and PAA and $\gamma_{PAA\text{-}air}$ between PAA and air. The term $1\text{-}\sigma$ describes the reduction of contact area between PS and external phase (water underneath the drop and PAA in the dry area) due to surface occupied by the grafting sites. These interfacial tension contributions are

classically found in the Young-Dupré equation. The additional term in Eq. 1 is the work W_{PAA}^{hyd} per unit area needed to bring a PAA chain from a dry state to its hydrated state in the brush. W_{PAA}^{hyd} can be expressed as the sum of two components $W_{PAA}^{hyd} = W_1 + W_2$, where W_1 corresponds to the hydration of a dry PAA chain by water at infinite dilution, and W_2 corresponds to the transfer of PAA chains from a solution at infinite dilution to a solution at the concentration of the brush. It is interesting to realize that W_2 is equivalent to the surface pressure of the corresponding diblock layer measured with the Langmuir trough at the deposition, *i.e.*$W_2 = \Pi$. As for W_1, it depends on the enthalpy of hydration of PAA and on the density of monomers per unit area as:

Eq. 2 $$W_1 = \Delta G_{PAA}^{hyd} \cdot \frac{d\, e_{AA}}{M_{AA}}$$

where ΔG_{PAA}^{hyd} is the free enthalpy of hydration of PAA per mole of monomer (at infinite dilution), M_{AA} is the molecular weight of a AA monomer, e_{AA} is the thickness of the PAA layer, and d is the density of PAA. Setting dW to zero in Eq. 1 and solving for θ leads the expression of the contact angle as:

Eq. 3

$$\theta = \arccos\left[\frac{1}{\gamma_{Air-H_2O}}\left((\gamma_{PAA-PS} - \gamma_{PS-H_2O})(1-\sigma) + \gamma_{PAA-Air} - \frac{\Delta G_{PAA}^{hyd} d e_{AA}}{M_{AA}} - \Pi\right)\right]$$

Total wetting is obtained if the work is negative even for $\theta = 0°$.

Eq. 4

$$\frac{\Delta G_{PAA}^{hyd} d e_{AA}}{M_{AA}} + \Pi \le \left(\gamma_{PAA-PS} - \gamma_{PS-H_2O}\right)(1-\sigma) + \gamma_{PAA-Air} - \gamma_{Air-H_2O}$$

Π, e_{AA} and σ are accessible experimentally for each sample by Langmuir trough and ellipsometry measurements. The interfacial tension $\gamma_{air/water} = 72$ mN/m is well established. The interfacial tension of polystyrene with water and air is subject to some uncertainty. We found $\gamma_{PS/air} \approx 40$ mN/m and $\gamma_{PS/H_2O} \approx 32$ mN/m in one set of publication[18,19] and $\gamma_{PS/air} \approx 29$ mN/m and $\gamma_{PS/H_2O} \approx 24$ mN/m in an other recent publication[20]. Note that the two set of values are consistent with the Young-Dupré equation for a water drop on bare PS making a contact angle with water of 83.5-86°. Since PS and PAA are strongly immiscible polymer, the interfacial tension $\gamma_{PS/PAA}$ can be estimated from the Flory parameter $\chi_{PS/PAA}$ between PS and PAA via the formula:

Eq. 5 $$\gamma_{PS/PAA} = 2\chi_{PS/PAA} k_B T / S_m$$

where $S_m \approx V_m^{2/3}$ is the area occupied by a monomer, and V_m is the molecular volume of a monomer. $\chi_{PS/PAA}$ is established in the literature at 0.4 [21]. Based on a density of PS of 1.05[22], the molecular volume for PS is $V_m \approx 165$ Å^3. For dry PAA in the protonated form, it is established in the literature that $V_m \approx 74$ Å^3. Eq. 5 supposes that PS and PAA have the same monomer size. Taking a median value of 120 Å^3, we find $\gamma_{PS/PAA} \approx 13.5$ mN/m. By comparison with other acrylate polymers, *e.g.* poly(n-butylacrylate) PBA ($\gamma_{PBA-air} \approx 31$ mN/m[18]), or poly(diethyleneglycol ethylether acrylate) PDEGA ($\gamma_{DEGA-air} \approx$ 33-35 mN/m[23]), the interfacial tension between PAA and air $\gamma_{PAA-air}$ can be estimated around 35 mN/m. In Eq. 3, ΔG_{PAA}^{hyd} is finally the only unknown. On Figure 11, the model fits satisfactorily the experimental data with a value ΔG_{PAA}^{hyd} = - 1200 to -1400 J/mol depending on the interfacial value γ_{PS/H_2O} that we use. These values corresponds to approximately ½ kT per monomer. As a comparison, it is possible to calculate ΔG_{PAA}^{hyd} from experimental data[24] of the molar fraction x_1 of water in PAA versus the partial pressure p_1 of water in the gas phase. The calculation is detailed in the annex and lead to ΔG_{PAA}^{hyd} = –1500 J/mol for a PAA sample of molar mass 4.10^3 g/mol. Given the imprecision in the determination of ΔG_{PAA}^{hyd} from the wetting data and from the hydration data, the consistency is quite remarkable. As ΔG_{PAA}^{hyd} is only dependant on the nature of the hydrophilic block and not on the molar mass of the sample, it is then interesting to apply the model to all polymer samples with ΔG_{PAA}^{hyd} = - 1300 J/mol. The results of the calculation that are reported on Figure 10. the model shows that the wetting is hardly dependant on the molar mass of the sample used. The curves for 4.3k-19.5k and 1.5k-44k are even undistinguishable. This is in good agreement with experimental observations. We have also checked that the role played by the area fraction σ occupied by the grafting site in the area of the transition is totally negligible. The maximum value of σ below the wetting transition for all samples remains below 0.04. In the calculation, the small influence of the molar mass on the wetting transition against the molar mass of the PAA chains comes from the internal surface pressure Π inside the brush. The term $\gamma_{PAA-PS} - \gamma_{PS-H_2O} + \gamma_{PAA-Air} - \gamma_{Air-H_2O} \approx$ -55 mN/m in Eq. 3 is much larger than the interfacial pressure Π at which the wetting transition occurs, *i.e.* around 3- 4 mN/m. This explains why the transition is hardly dependant on the length of PAA chains. With a less hydrophilic polymer than PAA, wetting transitions obviously occur at higher

amounts of polymer deposited. The relative importance of grafting sites area and internal pressure Π in Eq. 3 would then be larger, and the model predicts an important effect dependence of the molar masses of the grafted polymer on the wetting transition with e_{AA}. With a less hydrophilic polymer, other effects may have to be taken into account in the wetting properties. Cohen Stuart *et al.*[10] have studied the wetting of PEO brushes. They found an increase the hydrophilicity of substrates by PEO brushes but they never obtained a transition to total wetting. The authors have attributed this weak hydrophilization effect of PEO brushes to a bridging between the substrate and the air/water interface by grafted PEO chains. Indeed, PEO chains are well known for anchoring at an air/water interface[25]. In their view, this bridging effect retards spreading. Homogeneous and dense grafted monolayers of moderately hydrophilic chains that are able to promote a transition to total wetting would be a nice system to test further our model and the hypothesis of air/water surface bridging. We also note that our model predicts that layers of short molar masses PAA are less wetting than layers of large molar masses PAA, for a given PAA amount. This is opposite to the tendency observed with the advancing angles. This proves that the effect of the PAA molar mass on the advancing angles is not due to an average thermodynamic effect. The idea of a surface heterogeneity effect at the molecular scale, *i.e.* a carpet of short and dense hair against a carpet of scarce and long hair, is somehow comforted. It is interesting to comment our data in the light of Halpering and de Gennes[1] predictions. We confirm that a transition to complete wetting can be induced by grafting a polymer brush in good solvent conditions to a hydrophobic substrate. Whereas the transition in their case of neutral polymer was driven by the entropy of dissolution of the polymer, the transition with a polyelectrolyte is driven by both the entropy of dissolution of the polymer chains and the counter ions[26]. In spreading conditions, they predict the wetting film thickness versus the spreading coefficient S. However, they consider the case a non-volatile solvent and their predictions are not adapted to water, which is highly volatile. Experimentally, the study of the equilibrium thickness of a wetting film in total wetting conditions, would require a precise control of air humidity content, which was not done in this work. From a fundamental point of view, a wetting study of the same "hydrophobic-hydrophilic" surface by non volatile solvent would therefore be enlightening. One can think of a hydration transition versus e_{AA} in a water saturated atmosphere, since the physical condition driving hydration and wetting of a complex "hydrophilic-hydrophobic" surface are similar. A hydration study by X-ray reflectivity would permit to characterize the hydration properties and the eventual formation of hydration gradients in the polymer brush. By the same token, in order to complement the wetting study, it would be interesting to investigate the structure of the drop edge in the partial wetting conditions at a microscopic scale. It can not be discarded that a hydrated film forms ahead of the macroscopic edge, its growth being frustrated by evaporation.

4. Conclusion.

We have presented an experimental and theoretical study of the wetting by water of complex "hydrophobic-hydrophilic" surfaces made of a hydrophobic substrate covered by a highly hydrophilic polymer brush. For the preparation of model samples, we used polystyrene layers spin-coated on silicon wafers and covered with polystyrene-b-poly(acrylic acid) PS-b-PAA. The diblock copolymers layers were fabricated by Langmuir-Schaefer depositions and analyzed by AFM and ellipsometry. On poorly anchored layers, we observed large contact angle hystereses that have been attributed to nanometric scale dewetting of the polymer monolayer. On well-anchored monolayers, that form dense and flat brushes in the dry state, a wetting transition occurs versus the amount deposited. This confirms the prediction by Halperin and de Gennes [1] that a brush in good solvent condition can overcompensate the hydrophobicity of the underneath substrate and create total wetting conditions . We propose a model, that takes into account the finite concentration of the hydrophilic block inside the brush, through the air/water interfacial pressure Π of the brush and the free enthalpy of hydration the polyelectrolyte monomers ΔG^{hyd}_{PAA} . The originality and strength of the model is that all interfacial tensions between PS, PAA, water and air as well as the pressure in the brush Π can be measured or calculated. ΔG^{hyd}_{PAA} is the only fitting parameter and is the same for all grafting conditions (polymer length, grafting density). With ΔG^{hyd}_{PAA} = -1300 J/mol, the model renders the wetting transition for all samples and explains why, with PAA as hydrophilic agent, the wetting transitions depend mainly on the average thickness of the brush and weakly on the length of chains. We also found that this value of ΔG^{hyd}_{PAA} is remarkably consistent with determination based on PAA hydration experiments against water partial pressure, which reinforce the validity of the wetting model. In future work, it would be interesting to test the model with less hydrophilic polymer than PAA, for which the model predicts a significant (and therefore detectable) effect of the molar mass of the polymer on the wetting transition. The region in the vicinity of the edge drop remains to be investigated at the microscopic scale in order to get a better insight into the eventual hydration of the brush ahead of the drop and the role of evaporation of the solvent from this hydrated thin film.

Annex

The free Gibbs enthalpy of hydration of PAA at infinite dilution per mole of monomer ΔG_{PAA}^{hyd} can be extracted from experimental measurements of the molar fraction x_1 of water in PAA against the partial pressure p_1 of water in the gas phase. The chemical potential of the water is equal to :

Eq. 6 $$\mu_1 = \mu_1^0 + RT \ln\left(p_1 / p_1^0\right)$$

where μ_1^0 is the chemical potential of pure water. By application of the Gibbs-Duhem equation, the chemical potential of PAA μ_2 can be expressed as :

Eq. 7 $$\mu_2 = \mu_2^0 - RT \int_0^{x1} \frac{x_1}{(1-x_1)p_1} \frac{\partial p_1}{\partial x_1} dx_1$$

where μ_2^0 is the chemical potential of pure PAA. The change of Gibbs energy free when N_1 moles of water and N_2 moles of PAA are mixed is equal to :

Eq. 8 $$\Delta G_f = N_1\left(\mu_1 - \mu_1^0\right) + N_2\left(\mu_2 - \mu_2^0\right)$$

In order to get ΔG_{PAA}^{hyd}, one has to divide Eq. 8 by N_2 and take the value at $x_1 \approx 1$. This leads to:

Eq. 9 $$\Delta G_{PAA}^{hyd} = \left[\frac{x_1}{1-x_1} RT \, Ln\left(\frac{p_1}{p_1^0}\right)\right]_{X1\to 1} + RT \int_0^{x1} \frac{x_1}{(x_1-1)p_1} \frac{\partial p_1}{\partial x_1} dx_1$$

With a first order development of the logarithm term , we finally obtain :

Eq. 10 $$\Delta G_{PAA}^{hyd} = RT\left[-\partial \frac{\left(p_1/p_1^0\right)}{\partial x_1}\bigg|_{X1\to 1} + \int_0^{x1} \frac{x_1}{(x_1-1)p_1} \frac{\partial p_1}{\partial x_1} dx_1\right]$$

ΔG_{PAA}^{hyd} appears the sum of two terms, the left one being the contribution of water and the right term the contribution of PAA. Strictly speaking, at the limit $x_1 \to 1$, the term $\frac{\partial p_1}{\partial x_1}$ is necessarily null for the integral to converge and the left term due to water in Eq. 10 is necessarily null. In practice, we apply Eq. 10 and we calculate the derivative $\partial \frac{\left(p_1/p_1^0\right)}{\partial x_1}$ and $\frac{\partial p_1}{\partial x_1}$ by taking the difference $\Delta \frac{\left(p_1/p_1^0\right)}{\Delta x_1}$ and $\frac{\Delta p_1}{\Delta x_1}$ between the experimental point at the highest x_1 on Figure 13 and the theoretical point $x_1 = 1$ and $p_1/p_1^0 = 1$. In the limits of this approximation, we find ΔG_{PAA}^{hyd} =-1500 J/mol for a sample of molar mass M= 4.10^3 g/M (Figure 13).

Acknowledgements: We want to thank Rhodia, Inc. for financial and technical support, Thomas Gillet and Florence Coignet for participation to some of this work, JP Chapel for help with ellipsometry.

Tables

	h_{PS}	h_1	h_2^{PS}	h_2^{PAA}	Total thickness
Model 1	118.7	7.1	-	-	125.8
Model 2	118.7	-	121.3	4.0	125.3

Table 1: Thicknesses determined by ellipsometry of the PS subphase (h_{PS}) and of the deposited diblock layer by model 1 (h_1) and model 2 (h_2^{PS} and h_2^{PAA}) for a PS-b-PAA 1.8k-6k layer deposited at 21 mN/m.

List of Figures :

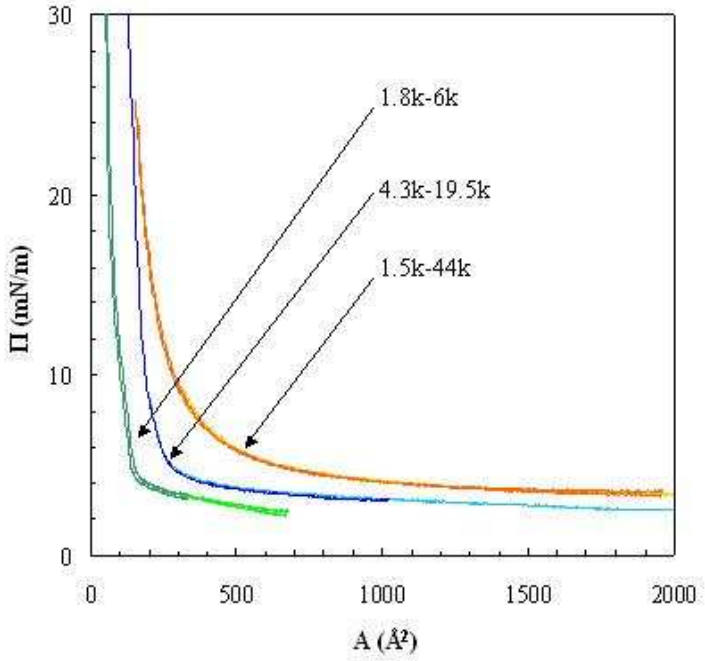

Figure 1: Isotherms of compression on pure water of PS-PAA diblock copolymers 1.6k-6k (green), 4.3k-19.5k (blue) and 1.5k-44k (orange). The amount of spreading solution is either 50 µL (light colors) or 100 µL (dark colors). The area indicated correspond to rw areas calculated from the amount of copolymer deposited.

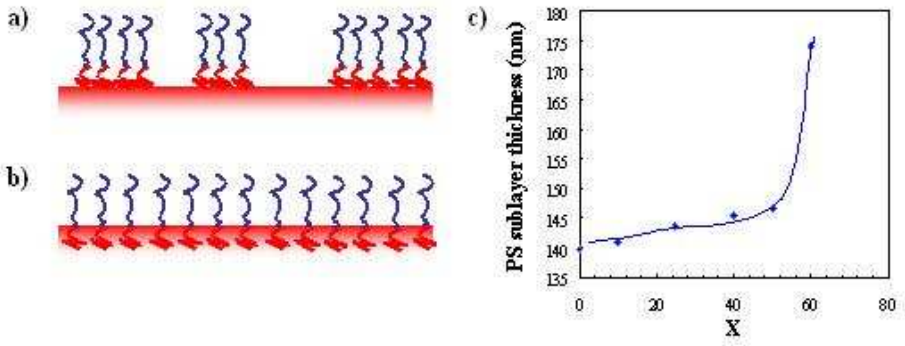

Figure 2: Schematic of PS-b-PAA copolymer chains a) deposited on PS without annealing, the chains can detach or move, b) after annealing, the chains are entangled and immobilized in the PS sublayer. c) PS sublayer thickness versus toluene composition X of toluene in water.

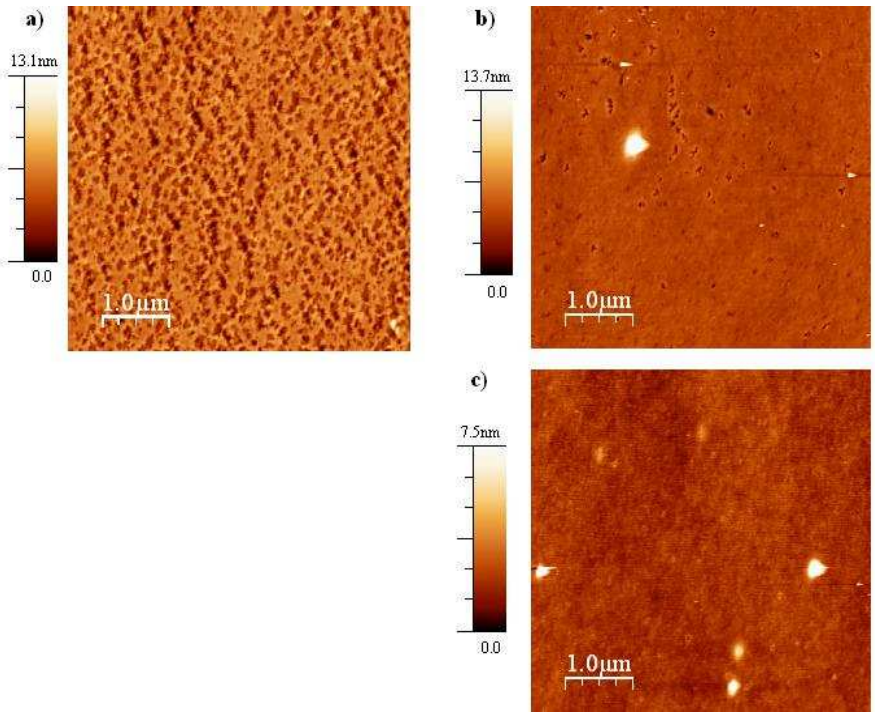

Figure 3: AFM images of PS-b-PAA 4.3k-19.5k monolayers deposited at 4.5mN/m.a) without annealing treatment – RMS Roughness = 1.50 nm, b) annealed by the toluene method- RMS Roughness = 0.86 nm, c) annealed by the temperature method - RMS Roughness = 0.67nm.

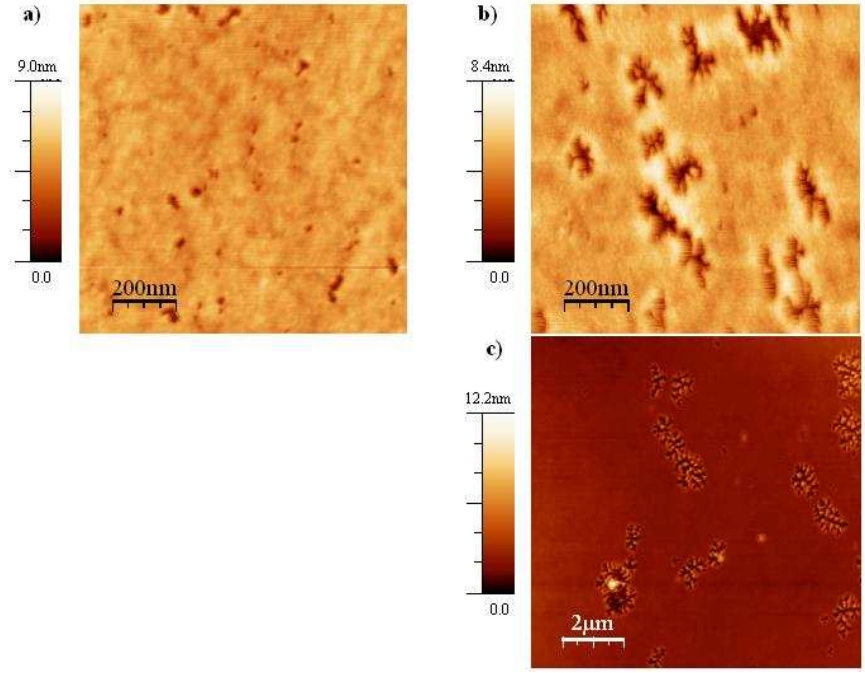

Figure 4: AFM images of PS-b-PAA monolayers deposited at 4.5mN/m and annealed by the toluene method: a) 1.8k-6k, holes: 3-5nm $e_{ellipso}$ =4.72 nm, b) 4.3k-19.5k, holes: 4-5nm $e_{ellipso}$ = 3.59 nm, and c) 1.5k-44k, holes : 3-4nm $e_{ellipso}$ = 3.66

nm.

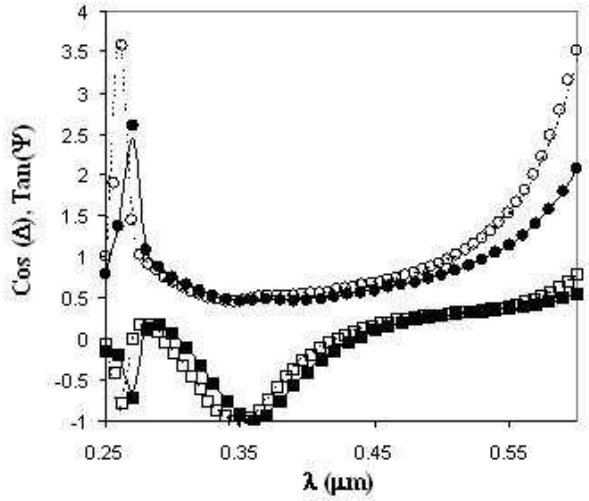

Figure 5: Ellipsometric data cosΔ (squares) and TanΠ (dots) before (hollow symbols) and after (dark symbols) deposition of a PS-b-PAA 1.8k-6k monolayer at Π = 21 mN/m. The lines corresponds to fits without (- - -) and with (——) the monolayer. The thickness of the PS substrate is found at 120 nm and of the PS-b-PAA monolayer at e = 7 nm.

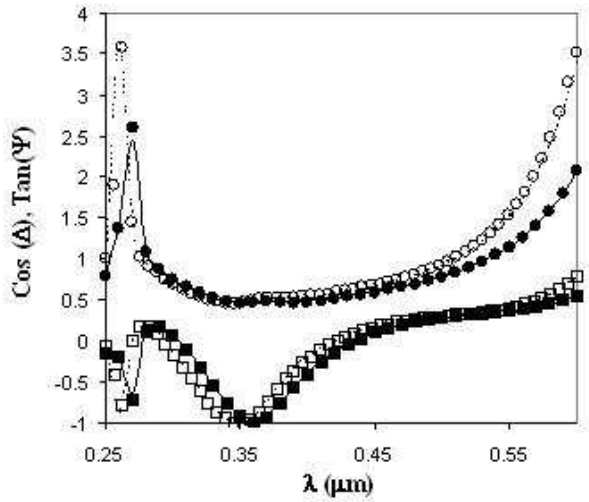

Figure 6: Ellipsometric thickness $e_{ellipso}$ versus Langmuir thickness $e_{Langmuir}$ calculated from the amount of copolymers spread at the air/water interface.

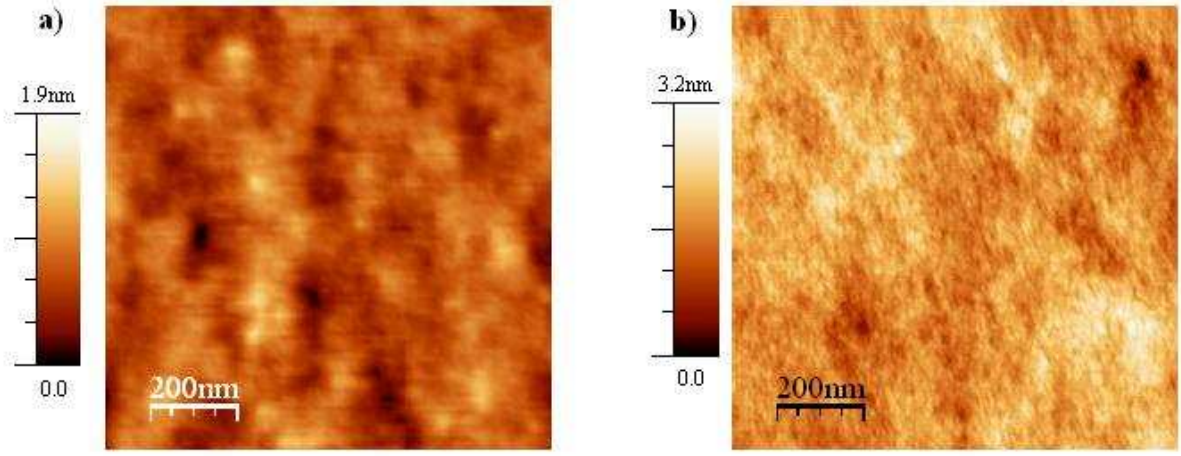

Figure 7: AFM images of PS-b-PAA 4.3k-19.5k monolayers after deposition and annealing a) deposition at Π = 21 mN/m, Rms Roughness = 0.27 nm, b) deposition at Π = 13 mN/m, Rms Roughness = 0.33nm.

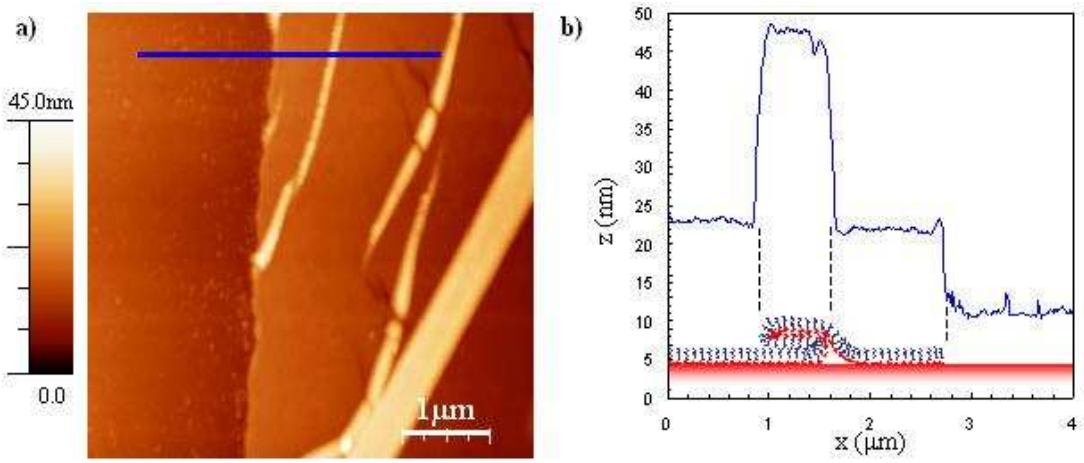

Figure 8: a) AFM image of PS-PAA 4.3k-19.5k layer deposited at 25 mN/m, 5µmx5µm and cracked, b) profile and cartoon of the organization of the copolymer chains at the surface.

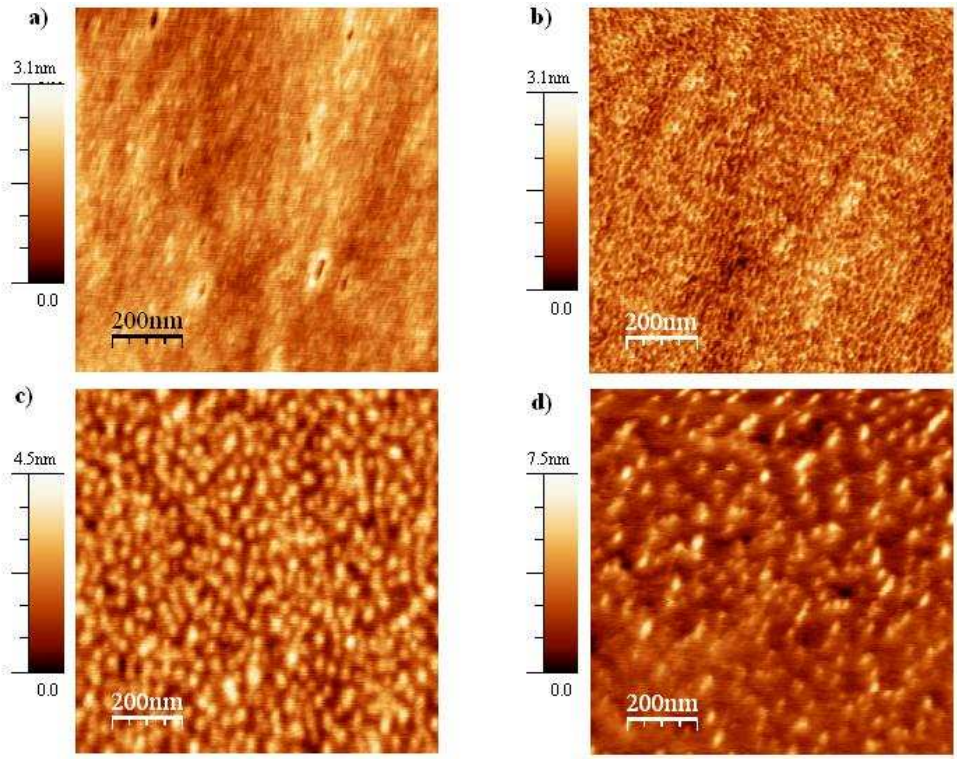

Figure 9: AFM images of PS-PAA 4.3k-19.5k layers deposited at a) 4.5mN/m, b) 2.5mN/m, c) 2.5mN/m:3, d) 2.5mN/m:5.

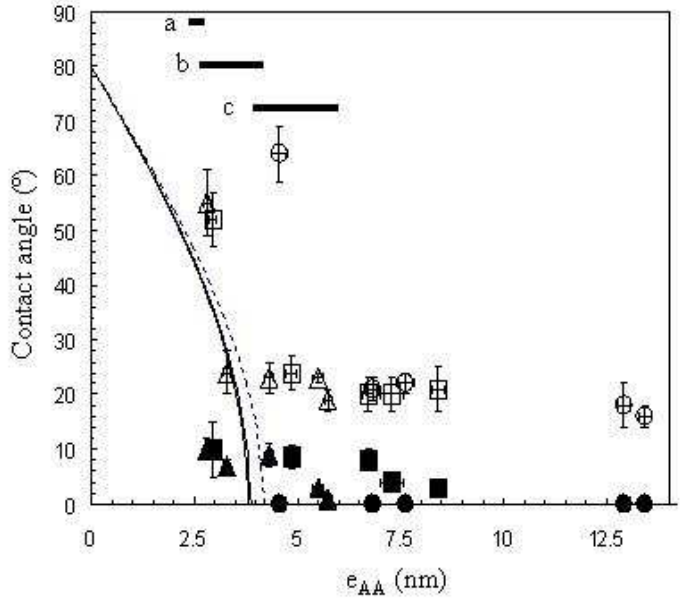

Figure 10: Water contact angles versus PAA thickness e_{AA} with samples annealed by the toluene method for PS-b-PAA 1.8k-6k (triangles▲ Δ), 4.3k-19.5k (squares □ ■) and 1.5k-44k (dots ● o). Hollow symbols correspond to advancing angles and full symbols to receding angles. The horizontal bars materialize the approximate position of the wetting transition observed with the advancing angles in the case of PS-b-PAA a) 1.8k-6k b) 4.3k-19.5k and c) 1.5k-44k. The lines correspond to fits by Eq. 5 with ΔG_{PAA}^{hyd} = -1300 J/mol for PS-b-PAA 1.8k-6k (- - -), 4.3k-19.5k (——) and 1.5k-44k (▬).

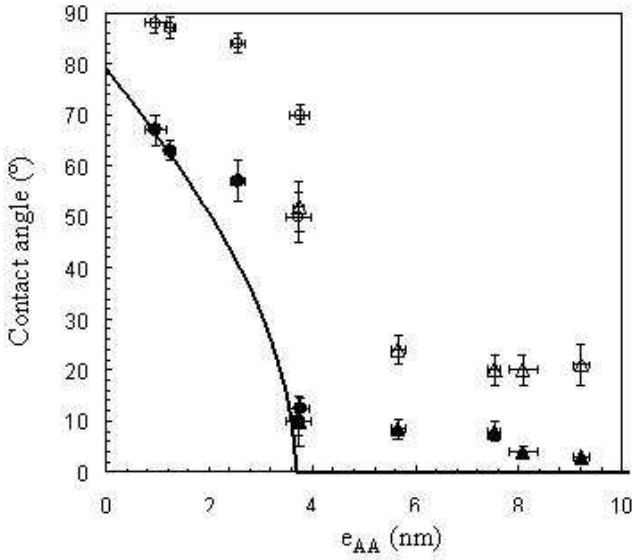

Figure 11: Wetting results –Contact angles versus PAA thickness for PS-PAA 4.3k-19.5k – Hollow symbols correspond to advancing angles and full symbols to receding angles. The data correspond either to samples annealed by the temperature method (circles) or the toluene method (triangles). The solid line corresponds to fits by Eq. 5 with ΔG_{PAA}^{hyd} = -1300 J/mol.

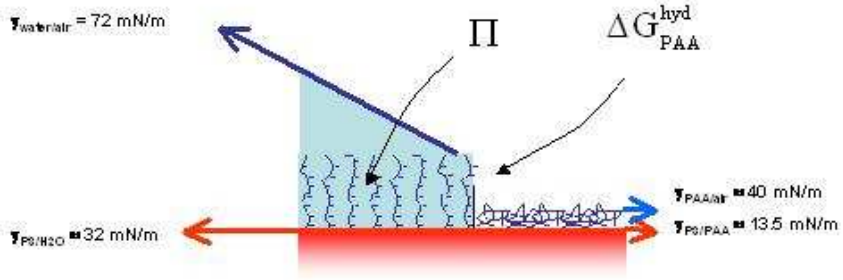

Figure 12: Illustration of the thermodynamic model, which takes into account the interfacial energies $\gamma_{PS/H2O}$, $\gamma_{H2O/air}$, $\gamma_{PS/PAA}$, $\gamma_{PAA/air}$, the enthalpy of hydration of AA monomers ΔG_{PAA}^{hyd}, and the interfacial pressure inside the brush Π.

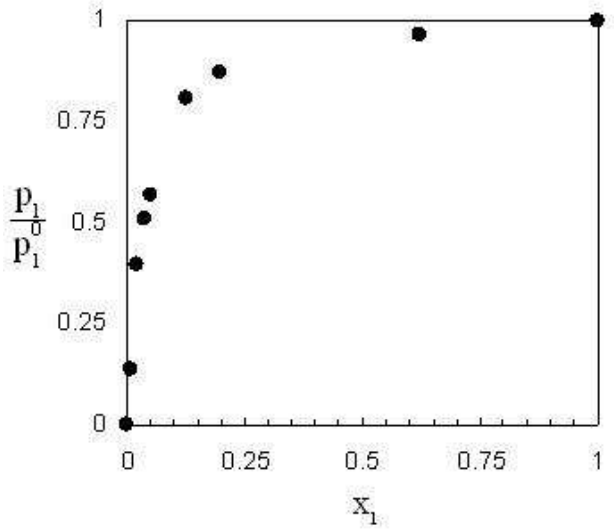

Figure 13: Experimental measurements of the molar fraction x_1 of water in PAA versus the partial pressure p_1 of water in the gas phase for a PAA of molar mass M= 4,000 g/M. These data have been published by Safronov et al.[24]

References:

[1] Halperin, A.; de Gennes, P.G. *J. Physique* **1986**, 47, 1243-1247.

[2] Leibler, L.; Ajdari, A.; Mourran, A.; Coulon, G.; Chatenay, D., Ordering in Macromolecular Systems, A. Teramoto, M. Kobayashu, T. Norisuje 5Eds.), Springer-Verlag Berlin Heidelberg, **1994**.

[3] Maas, J. H.; Fleer, G. J.; Leermakers, F. A. M.; Cohen Stuart, M. A. *Langmuir* **2002**, 18, 8871-8880.

[4] Liu, Y.; Rafialovich, M. H.; Sokolov, J.; Schwarz, S. A.; Zhong, X.; Eisenberg, A.; Kramer, E. J.; Sauer, B. B.; Satija, S. *Phys. Rev. Lett*. **1994**, 73, 440-443.

[5] Gay, C. *Macromolecules* **1997**, 30, 5939.

[6] Kerle, T.; Yerushalmi-Rozen, R.; Klein, J. *Macromolecules* **1998**, 31, 422-429.

[7] Reiter, G.; Auroy, P.; Auvray, L. *Macromolecules* **1996**, 29, 2150-2157.

[8] Johner, A.; Marques, C.M. *Phys. Rev. Let.* **1992**, 69, 1827-1830.

[9] Ramdane, O.O.; Auroy, P.; Silberzan, P. *Phys. Rev. Let.* **1998**, 80, 5141-5144.

[10] Cohen Stuart, M.A.; de Vos, W.M.; Leermakers, F.A.M *Langmuir* **2006**, 22, 1722-1728.

[11] Roberts, G., Ed. Langmuir-Blodgett Films; Plenum Press: NewYork, **1990**.

[12] O. Gareil, T. Futterer, O. Theodoly, P. Muller, Compression isotherms of charged diblock copolymers, to be submitted.

[13] Valignat M.P., Theodoly O., Crocker JC, Russel W.B., Chaikin PM. *Proc. Natl. Acad. Sci.* **2005**, 102, 4225-4229.

[14] Theodoly, O.; Checco, A.; Ocko, B.; Muller, P. A GISAXS study of PS-b-PAA at the air/water interface, to be submitted.

[15] Young, T. Philos. Trans. R. Soc. London **1805**, 95, 65.

[16] Dupré, A. Théorie mécanique de la chaleur,; Gauthier Villars; Paris, **1869**; pp369.

[17] Adam, N. *Nature* **1957**, 180, 809.

[18] S. Wu, surface and interfacial tension of polymers, oligomers, plasticizers and organic pigments, Polymer Handbook, Fourth Ed., Editors: J Brandrup, E.H. Immergert, E.A. Grulke.

[19] Takashi, S.; Shimizu, A. ; Mourey, T.H. ; Thureau, C.T. ; Ediger, M.D. *J. Chem. Phys*. **2003**, 119, 16, 8730.

[20] Li,Y.; Pham, J.Q.; Johnston, K.P. ; Green, P.F. *Langmuir* **2007**, 23, 9785-9793.

[21] Bendejacq, D.; Ponsinet, V.; Joanicot, M.; Vacher A.; Airiau M. *Macromolecules* **2003,** *36*, 7289-7295.

[22] Brandrup, J. ; Immergut, E. H. ; Grulke E. A. Polymer Handbook 4th edn, Wiley Interscience, New York, **1999**.

[23] We measured these values by drop shape analysis in water of homopolymer PDEGA drops of molar mass ranging from 3kD to 30 kD.

[24] Safronov, A.P.; Tager, A.A.; Klyuzhin, E.S.; Adamova, L.V. *Polymer Science* **1993**, 35, 6, 818-821. Translated from Vysokomolekulyarnye Soedineniya, Ser A, Vol. 35, No. 6, 1993, pp. 702-706.

[25] Barentin, C.; Muller, P.; Joanny, J.F. *Macromolecules* 1998, 31, 7, 2198-2211.

[26] The ionization state of PAA chains in a brush exposed to pure water is intermediate between the state in a brush exposed to pH 11 aqueous solution (full ionization) and pH 2 aqueous solutions (no ionization).